Advanced Control Approach for Hybrid Systems Based on Solid Oxide Fuel Cells

M. L. Ferrari
Thermochemical Power Group (TPG)
Dipartimento di Macchine, Sistemi Energetici e Trasporti (DIME)
Università di Genova, Italy
mario.ferrari@unige.it

Abstract

This paper shows a new advanced control approach for operations in hybrid systems equipped with solid oxide fuel cell technology. This new tool, which combines feed-forward and standard proportional-integral techniques, controls the system during load changes avoiding failures and stress conditions detrimental to component life. This approach was selected to combine simplicity and good control performance. Moreover, the new approach presented in this paper eliminates the need for mass flow rate meters and other expensive probes, usually required for a commercial plant. Compared to previous works, better performance is achieved in controlling fuel cell temperature (maximum gradient significantly lower than 3 K/min), reducing the pressure gap between cathode and anode sides (at least a 30% decrease during transient operations), and generating a higher safe margin (at least a 10% increase) for the Steam-to-Carbon Ratio.

This new control system was developed and optimized using a hybrid system transient model implemented, validated and tested within previous works. The plant, comprising the coupling of a tubular solid oxide fuel cell stack with a microturbine, is equipped with a bypass valve able to connect the compressor outlet with the turbine inlet duct for rotational speed control. Following model development and tuning activities, several operative conditions were considered to show the new control system increased performance compared to previous tools (the same hybrid system

model was used with the new control approach). Special attention was devoted to electrical load steps and ramps considering significant changes in ambient conditions.

Keywords

Control system, SOFC hybrid system, feed-forward technique, PI controller.

1. Introduction

Hybrid systems, consisting of a solid oxide fuel cell (SOFC) combined with a microturbine (mGT), are expected to have a significant role due to widespread distributed generation paradigm [1-4] and hydrogen economy [5-7]. More specifically, high performance aspects in small-size systems (ultra-high efficiency [8,9], ultra-low emissions [10], fuel flexibility [11,12] and co-generative applications [13,14]) of these innovative plants are essential in terms of environmental and energy demand [15,16].

Despite the important results obtained for SOFC hybrid systems through both theoretical [17-19] and experimental [8,20,21] tools, only one prototype, developed by Siemens-Westinghouse [22], reached performance levels close to the expectations. This low rate of success for these kinds of plants is due to the high cost of components [7,23] and technical problems related to system integration [7,24,25]. An important technical issue not completely settled concerns the control system because SOFC hybrid plants are subject to several additional constraints as opposed to standard mGT plants [26]. More specifically, in addition to turbine constraints (maximum rotational speed, surge line and maximum thermal stress for components [27]), other risk situations must be addressed [26,28], including (I) excessive temperature or (II) thermal gradient in the fuel cell, (III) excessive pressure difference between cathodic and anodic sides and (IV) too low Steam-To-Carbon Ratio (STCR) in the SOFC anodic side. These constraints must be considered not only for steady-state conditions, but also during time-dependent operations [29], such as load variations, ambient temperature changes and start-up/shutdown phases [30]. More specifically, several challenges must be overcome to couple the very fast response of the mGT system (low mechanical inertia of the turbine shaft) with the slow thermal variations of the SOFC stack [31] (high thermal capacitance of fuel cell materials), while the different volume values of SOFC sides generate different time-dependent performance in terms of pressurization/depressurization delays (an important aspect to take into account in order to prevent excessive cathode/anode pressure difference during transient operations [25]). Moreover, the fluid dynamic and chemical responses of the anodic side, important aspects to avoid low STCR values, are usually not in line with the transient behaviour necessary to prevent other failures [32-34].

Although in the last ten years several works [29,33,35-37] have been carried out on these control issues, the problem is not completely solved due to the large number of constraints to be considered and aspects related to costs that have not been completely optimized. For instance, even if some papers [33,36,37] presented effective control systems for SOFC hybrid plants, thermal stress on the fuel cell was not always prevented (significant thermal gradient: higher than 3 K/min [38] especially for large load steps) and expensive probes were used (e.g. mass flow rate meters in [33,35]). Moreover, the cathode/anode pressure difference was carefully considered only in [33], while other control systems showing interesting result neglected the constraints of this important property (see [26] for experimental aspects). Also the time-dependent aspects related to anodic recirculation were often neglected (considering constant recirculation ratios [38]) or based on very simple approaches [37]. Since the importance of anodic circuit response is essential in preventing failures (e.g. low STCR), it is imperative to develop a transient model of the anodic devices (e.g. an anodic ejector [26,39]) to study a reliable control system for the entire plant [33].

This work focused on the development of an advanced control system for SOFC hybrid plants. So, the control strategy presented in [33] was improved considering the coupling of Proportional-Integral (PI) controllers with feed-forward approaches to prevent thermal stress in the fuel cell and to reduce the peak values of cathode/anode pressure difference and STCR. Since the thermal capacitance of the stack is very high, the PI controller necessary to maintain constant stack temperature must be a very slow response device (as done in [33]) to avoid unstable behaviour. However, this approach cannot prevent significant thermal gradients (higher than 3 K/min) in the fuel cell (responsible of serious stress on ceramic material) because the new rotational speed set-point is generated only after an excessive temperature oscillation. On the other hand, the coupling with feed-forward technique (in a system equipped with load variation smoothing devices: a battery package or an electrical grid) can obtain the new rotational speed with the requested time performance and without instability problems. Moreover, this is a simple approach (in comparison with multiple-input and multiple-output controllers), which can combine possible corrective actions for disturbances (e.g. variations of ambient conditions) with less oscillations in plant critical properties. Even if the same basis shown in [33] was maintained (e.g. the mGT speed control was carried out with a compressor/turbine bypass valve), the results obtained with a Matlab®-Simulink® transient model shows better performance in terms of thermal and mechanical stress on the components. The Matlab® version used in this work is the R2010a (7.10.0.499), which is coupled with version 7.5 of the Simulink® tool.

This work demonstrates improved control performance, over previous works [29,32,33,41], which can prevent failures and increase component life, also broadening the types of transient operations (e.g. variations of ambient conditions) carried out with a previously validated model [42,43].

2. Plant Layout and Control System

The hybrid system considered in this work (continuous lines in Fig.1) is based on Siemens-Westinghouse [22,33] technology for a global size in the range of 300 kW. The plant layout comprises the coupling of a tubular pressurized SOFC with a recuperated microturbine. On the cathodic side air is compressed by a radial machine, preheated by the recuperator and fed to the fuel cell, while in the anodic ducts fuel (methane) is converted into a hydrogen rich mixture by a reformer unit located upstream of the stack. The anodic side is based on a recirculation system carried out by a single-stage ejector: methane is pre-heated with the plant exhaust flow and fed into the ejector primary duct, while a part of the SOFC exhaust (anodic flow) is recirculated by the ejector (secondary nozzle). The flow comprising the mixture of this recirculation and methane is fed to the stack anodic side. Finally, the anodic circuit outlet flow is mixed with the cathodic exhaust flow in the off-gas burner to increase turbine inlet enthalpy. The expander can produce the power needed for the compressor and an useful power additional to the fuel cell generation. On the electrical side the system is equipped with a battery package in case of stand-alone operation mode (in case of grid connected operations, the electrical grid can substitute the battery function). The main property values of the plant at design conditions are reported in Tab.1.

Table 1. Design values of main plant properties.

Net electrical power of the entire hybrid system [kW]	284.8
Stack electrical power [kW]	231.3
Net electrical power of the turbine [kW]	53.5
Power consumed by the fuel compressor [kW]	9.4
Global net electrical efficiency [-]	0.637
Fuel utilization factor	0.85
Current density [mA/cm^2]	423.9
Stack average temperature [K]	1229.8
Fuel mass flow rate in the ejector primary duct [kg/s]	0.009
Anodic ejector recirculation ratio [-]	7.18
Air mass flow rate [kg/s]	0.658
Compression ratio [-]	3.85
Recuperator effectiveness [-]	0.89
Turbine inlet temperature [K]	1080.1
Turbine outlet temperature [K]	847.6
Shaft rotational speed [rpm]	68000

The control strategy considered in this work is shown in Fig.1 using dotted lines. It is based on the coupling of standard PI controllers (as in [33]) with a feed-forward technique. The latter approach is necessary to prevent the high thermal gradient values shown in [33] and in other previous works (e.g. in [38]). Since the stack thermal capacitance is very high, a possible simple solution to avoid temperature oscillations (and thermal gradients higher than 3 K/min) is the application of the feed-forward technique (based on interpolation tables) because it can obtain the requested rotational speed change without the unstable behaviour typical of a feedback-based controller. However, this new approach can produce the expected performance if load variation is smoothed by a battery or an electrical grid. The numbers of control lines is selected in accordance with [33]. For this reason, where this new approach allows removing a control line in comparison with [33], the related number is not used. This layout is based on a bypass valve for direct connection between the compressor outlet and the turbine inlet ducts. This approach (proposed in [33]) is necessary to control the mGT rotational speed (point 1 in Fig.1) solving the issue related to the difference between the small mechanical inertia of the microturbine shaft and the very high thermal capacitance of the fuel cell stack. While the fractional opening (FO) design value is low (0.05) to achieve good efficiency in steady-state conditions, this valve is managed by a PI controller to maintain the mGT rotational speed at its set-point value.

The system input is the power demand (point 2) for the entire plant. The actual power requirement is calculated considering a control device capable of smoothing the input variations with a battery package as in Fig.1 or through the electrical grid. Also in this work the electrical dumper is controlled by a PI equipped with a previous step block (see Fig.2 for details) capable of reducing power change effects; different solutions are available. The coefficient of the integral part of this PI is calculated through an interpolation table on the basis of the bypass valve FO (this approach is necessary to reduce fuel cell pressure difference by decreasing the response speed of power variation smoothing when FO is significantly different from its design value). Then, the power requested to the SOFC is calculated by multiplying the input signal by a sharing-out coefficient (point 3) as presented in [33]. However, unlike [33], an initial improvement is obtained through a feed-forward approach used to evaluate this coefficient to keep the bypass valve set-point value at 0.05. Instead of a slow response PI controller [33] being responsible for a very significant FO oscillation (linked with a cathode/anode pressure difference high peak), a table of data coming from steady-state analysis is interpolated on the basis of the hybrid system power demand, ambient conditions, anodic recirculation temperature and fuel temperature. The SOFC power demand (point 5) is used to evaluate stack current (point 7) calculated by a fast response PI controller. This control device operates to nullify the difference between the SOFC power demand and the effective power generated by the fuel cell (point 6). The remaining electrical demand (point 8) is satisfied by the mGT generator. Fuel flow rate is managed by a valve located upstream of the ejector primary ducts whose FO value (point 12) is calculated through a second feed-forward controller (a second table of data interpolated on the basis of the hybrid system power demand, ambient conditions, anodic recirculation temperature and fuel temperature), instead of a PI device as carried out in [33]. With this new approach, it is possible to keep constant (0.85 at off-design conditions) the fuel utilization factor inside the SOFC, avoiding an expensive fuel mass flow rate probe (necessary device to operate as in [33] with a slow-response PI). Moreover, this second feed-forward controller can significantly reduce the fuel utilization factor oscillations in comparison to the results obtained in [33]. A final controller is necessary to maintain constant SOFC average temperature value. Also in this case, a feed-forward approach is used to calculate the rotational speed set-point (point 11), replacing the slow response PI controller proposed in [33]. This control type change is necessary to avoid significant oscillations in SOFC average temperature, which can generate dangerous thermal stress on ceramic material (especially with thermal gradient values higher than 3 K/min [40]). To ensure the flexibility needed to achieve the response of this controller, the table of data interpolation (including the effects of ambient condition, anodic recirculation temperature and fuel temperature) is carried out including a delay for the hybrid system power demand. This delay unit is based on a slow-response PI controller where the plant power demand is operated as a set-point and the controller output is used as a feedback signal input (see Fig.2 for details). The complete diagram of a PI controller coupled with a previous step block is shown in Fig.2. This configuration can operate as a delay (including the proportional part) of the input value because the previous step block generates the PI set-point value equal to the PI output calculated during the previous calculation step. It also includes an optional input line that is used when it is necessary to change the integral part coefficient. At steady-state condition the output value converges with the input value. This solution was selected instead of a transfer function to utilize similar control devices within the system, thus simplifying the approach: just PI controllers, interpolation tables and algebraic blocks. However, the same effect can be obtained with a first-order transfer function.

The values implemented in the interpolation tables shown in Fig.1 were obtained by steady-state calculations carried out considering different values in plant power demand and other influence properties (the main results of this steady-state analysis was reported in [44]) or (for the coefficient factors related to the PI integral part for battery management) from preliminary simulations. The typical limitation of the feed-forward approach (no corrective actions from disturbances) was solved including interpolation table variation (with apt corrective factors) in case of variations of measurable disturbances (ambient conditions, fuel temperature and fuel composition). For this reason Fig.1 includes the following inputs: ambient conditions (temperature, pressure and humidity), fuel temperature and anodic recirculation temperature (its variation can show the effect of fuel composition variation to be compensated in the interpolation tables). Moreover, the not measurable disturbances (e.g. degradation of plant components) can also be compensated with the same approach. In this case, it is necessary to use available measurements to detect the degradation (and the degradation level). For instance, the stack degradation can also be detected by anodic recirculation temperature. In this case, feed-forward components can be adapted modifying the interpolation tables on the basis of this property, maintaining, also in case of stack degradation the target temperature value of the SOFC.

3. Model

The control system development and testing were carried out with a transient model implemented in Matlab®-Simulink® environment. Although in this work the control system is completely new, the same models of [33] were considered for plant components to highlight the good performance achieved by this new control system compared to the previous one [33]. This model was developed using the TRANSEO tool [45,46], a visual, user-friendly modular program based on a library of components for off-design, transient and dynamic analyses [47] of energy systems.

The modelling technique for the main part of the plant components is based on a 0-D approach (balance equations integrated just between inlet and outlet of devices) called "lumped volume". Each component (except the recuperator that is based on a quasi-2-D technique [47]) is modelled with an off-design calculation software connected to a constant section pipe model for fluid dynamic delay [44]. This simplified approach is essential to reach reasonable computational time, ensuring that calculation performance is satisfactory for plant level simulations, as demonstrated in several previous validation works carried out with this modelling technique [42,43]. More specifically, 0-D approaches were demonstrated [19,32,33] to be very effective in control system development and assessment. As stressed in [33,45], models of all plant components include thermal loss and transient response related to changes in chemical composition.

3.1 Fuel Cell Model

This paper is based on a fuel cell tubular geometry, similar to the design proposed in [33,45], and on surrounding facilities (reformer, pre-heating tube, anodic recirculation, etc.) connected as presented in [49]. The fuel cell model is based on the following hypotheses: adiabatic, uniform voltage, chemical reactions at equilibrium, CO electrochemical reaction neglected. As presented in [50], the fuel cell model includes: voltage calculation subtracting ohmic and activation losses from Nernst's potential, equilibrium of reforming and shifting chemical reactions, mass balances of anodic and cathodic flows (including the effect of reactions), energy balances of flows (this calculation includes: the anodic gas, the flow within the pre-heating quartz tube and the cathodic air, the energy balance related to the tube and the solid PEN (positive(P)-electrolyte(E)-negative(N)) structure. A time-dependent first-order differential equation is used to calculate the stack material average temperature considering thermal balances and the total stack thermal capacitance.

This model was validated at stack level considering a wide result comparison against a detailed 1-D model (previously validated against experiments) in both steady-state and transient conditions [50]. The assessment presented in [50] showed that the 0-D approach used for the fuel cell model can generate reliable results for plant level analysis and control system development.

3.3 Models for Plant Components

Special attention was devoted to the ejector transient model. It was developed in previous works [42,45,46] and validated against experimental data at both steady-state and transient conditions [42]. Given the importance of this component for the anodic side performance [51-53], a detailed validation was carried out for recirculation systems using experimental data obtained through reduced-scale emulator rigs [42,54].

Models for the compressor and turbine are based on the interpolation of characteristic non-dimensional curves. Although this is a typical approach for these kinds of machines [55-57], several previous works [45-48] carried out with TRANSEO tool validated these models in transient operations too. The recuperator model is based on a quasi-2D approach to achieve reliable results. Previous works [46,48,58] demonstrated that this technique based on 10 calculation nodes is a good compromise between result performance and computational time. Moreover, the recuperator model was validated against experimental data in [48,58].

Finally, validation activity was carried out at system level using the hybrid system emulator rig of the NETL - U.S. DOE located in Morgantown (WV). This plant was able to validate all the cathodic-side models (compressor, turbine, shaft, generator, recuperator, cathodic volume and off-gas burner) at both steady-state and transient conditions [43].

4. Results

To compare the performance obtained with this new control system to the results obtained in [33], initial simulation tests were carried out considering a 10% load step decrease and a 5% load step increase. In both cases, the same hybrid system model shown in [33] was used to perform a control system comparison. Then, the new control system was used to analyse the effect of changes in ambient conditions in conjunction with electrical load ramps (to simulate real plant operations).

4.1. Load Step Decrease

This paragraph presents a simulation carried out with the model using the new advanced control system based on the interpolation tables shown in Fig.1: a feed-forward (FF) approach is implemented for some controllers. To compare the results to the performance obtained with a previous PI based control system [33], a 10% load step was considered (as in [33]) for the entire hybrid plant: from about 284.8 kW to 256.3 kW at constant ambient conditions (air at 60% relative humidity, 288.15 K temperature and 1.013 bar pressure). Many simulations were carried out before obtaining the results presented here. This preliminary work was necessary to implement the parameter values especially for the coefficient table of the battery PI controller and for the response of the rotational speed set-point calculator. The results shown in [33] (for PI coefficients coming from Ziegler-Nichols technique [59] followed by a significant tuning activity) were a starting point to maintain the controller in stable condition. However, in this work, extensive activity based on trial-and-error technique was carried out to improve results. More specifically, it was very difficult to synchronize the very different dynamics of the following parameters: fuel cell load, turbine rotational speed and fuel mass flow rate. For instance, to maintain constant SOFC average temperature (with maximum gradient lower than 3 K/min) it is necessary to adapt turbine rotational speed as quickly as load changes on the stack. However, a strong limitation is present to avoid an excessive large bypass valve (decreasing plant efficiency) or surge problems. For this reason, high temperature gradients were not prevented in [33,38]. Moreover, the different anodic loop dynamics (mainly due to the different volumes of the cell sides) can generate excessively high differential pressure values if fuel flow rate is not changed with the same time scales. Unfortunately, if this mass flow rate variation is carried out too quickly (especially in case of load increase) the constraint related to the STCR parameter is not satisfied, generating values lower than 1.8 during the transient operations. So, the battery controller was tuned to obtain the fastest possible response and to reach a compromise between battery operation time decrease (linked with cost decrease due to limited installation of battery components due to maximum power decrease requested by this component) and system, operated in accordance with the various constraints (including the SOFC time-dependent thermal gradient constraint, usually neglected in several previous works [38]).

The global management of the plant obtained with the control system is shown in Fig.3. Since the electrical demand (for the whole hybrid system) is decreased by the 10% step at time 0 of Fig.3, the battery package is used to smooth this load decrease: both SOFC and mGT can slowly reduce slowly their load values, while the additional power produced by the plant is absorbed by the battery (negative power means battery re-charging phase). However, if the plant can be connected to an external electrical grid, the same behaviour (same power variation smoothing) can be obtained without battery costs. Since the battery smoothing effect has a time response longer than the thermal one (mainly due to the SOFC high thermal capacitance), the effect of fluid dynamic response (also including pressurization/depressurization volume response) is negligible in the results presented in this work. Furthermore, as shown in Fig.4, the rotational speed oscillation typical of load step response (as shown in [33]) is also not present because load demand variation on the mGT is smoothed by the battery. Figure 4 also includes fuel cell inlet pressure at the cathodic side (downstream of the air pre-heating tube) showing a pressure decrease trend due to rotational speed decrease. These trends, compared to the results obtained in [33] (see Fig.4), show a slow-response decrease due to a slow decrease in rotational speed set-point (signal 11 in Fig.1) driven by the PI connected to a previous step block. This approach is necessary to produce a proper delayed response to keep constant the SOFC temperature (Fig.5). The good performance of this controlling solution is well demonstrated by Fig.5 because SOFC average temperature is maintained almost constant (0.7 K maximum variation during this test) and time-dependent temperature gradient is almost negligible. The load change smoothing obtained using the battery and the good rotational speed set-point calculation carried out through the feed-forward (FF) approach can avoid significant SOFC temperature oscillations. This is a significant improvement considering that the previous solution [33] based on a PI controller generated a high temperature maximum gradient (about 10 K/min) usually not sustainable by the fuel cell stack.

During the test, the sharing-out coefficient (Fig.6) and the fractional opening (Fig.7) of the bypass valve show decreased oscillating behaviour and a slower response variation compared to the results reported in [33]. Also their trends are due to the battery smoothing effect coupled with a feed-forward approach for the sharing-out coefficient calculation too. Using the interpolation table (instead of the PI controller shown in [33]) to calculate this coefficient value is an effective solution to maintain the 0.05 fractional opening value at steady-state condition, avoiding efficiency (defined in Eq.1) decay due to high mass flow rate bypassed from compressor to turbine. The good performance obtained with this new control system is shown by the plant net efficiency (Fig.8). In comparison with results calculated in [33], it is possible to avoid significant efficiency decays at transient condition too.

$$eff = \frac{P_{FC} + P_{mGT} - P_{aux}}{m_{fuel} \cdot LHV} \tag{1}$$

$$U_f = \frac{\left[n(H_2) + 4 \cdot n(CH_4) + n(CO)\right]_{FC\_in} - \left[n(H_2) + 4 \cdot n(CH_4) + n(CO)\right]_{FC\_out}}{\left[n(H_2) + 4 \cdot n(CH_4) + n(CO)\right]_{FC\_in}} \tag{2}$$

The performance obtained with the interpolation table needed to manage the fuel valve is reported in Fig.9. Both current and fuel mass flow rate decreases are slower in comparison with previous results [33] because the battery can smooth the load change on the fuel cell. This approach allows maintaining almost constant fuel utilization value (see Eq.2 for its definition) with 1% maximum decay during the transient response (reaching the 0.85 design value at steady-state condition). This behaviour is significantly different from the results discussed in [33] where a 17% U_f decay is shown immediately after the 10% load decrease step.

As mentioned in the Introduction, an effective control system for hybrid plants must be able to prevent critical values also for the following parameters: STCR, anode-cathode differential pressure, Turbine Inlet Temperature (TIT) and compressor surge margin. Even if it is very difficult to maintain all these parameters within the constraints during time-dependent operations, the smoothing effect of the battery coupled with the feed-forward technique can produce the requested performance. So, the new control approach presented in this paper compensates for the different dynamics responsible for possible critical conditions during transient operations. More specifically, Fig.10 shows that this new control system can prevent low STCR (see Eq.3) values and non-sustainable fuel cell differential pressure. In comparison with results shown in [33], it is possible to obtain smaller variations increasing the possible plant operation field (larger load steps are acceptable) and to reduce mechanical stress on the stack. The maximum peak of differential pressure value is significantly reduced (maximum peak absolute value from 17.6 mbar to 9.4 mbar) using this new control system based on interpolation tables (feed-forward approach for three parameters). For the other critical properties (TIT and Kp), Fig.11 shows that this new control system can prevent TIT peaks and surge conditions. In comparison with [33], the behaviour is less oscillating also for TIT and surge margin (see Eq.4 for its definition). However, no significant thermal stress is generated by this load step (larger steps can be acceptable) because the TIT design value has a significant safety margin (higher than 100 K for standard commercial mGTs) and the temperature increase shown in Fig.11 is very small (about 5 K). Moreover, surge risk is prevented because Kp parameter significantly increases in comparison with its design value.

$$STCR = \frac{n(H_2O)}{n(CO) + n(CH_4)} \tag{3}$$

$$Kp = \frac{\beta_{s.l.} \cdot m}{\beta \cdot m_{s.l.}} \tag{4}$$

Another important aspect to check in these kinds of plants is chemical stress on the fuel cell due to significant chemical composition variation. For this reason, Fig.12 shows mass fractions of the anodic outlet flow (upstream of the off-gas burner) referenced to their design values (each mass fraction is divided by its design value to better show the time-depended variation). The design values are: 0.518 for CO_2, 0.004 for H_2, 0.438 for H_2O and 0.040 for CO. To better present the performance obtained with this new control system, attention is focused (Fig.12) on the results obtained with the feed-forward (FF) approach. The chemical composition variation was maintained fairly constant because the variations of mass fractions were always lower than 5%. Moreover, for the most significant components (CO_2 and H_2) in the flow, Fig.12 shows a variation lower than 0.4%. Similar stable performance was obtained on the cathodic side (with a plot not shown here for sake of brevity).

To complete the evaluation of this new control system performance, the same simulation (10% load step decrease) was carried out removing the battery (or the connection to an electrical grid) from the system. In comparison with [33] (based on just feedback technique for all the controllers), the results obtained in this case showed a better control of SOFC average temperature (4 K oscillation instead of 29 K obtained in [33]) for the application of the feed-forward approach. However, some parameters are significantly critical: anode-cathode differential pressure reached 77 mbar at the beginning of this transient operation, STCR showed an excessively large oscillation (from 2.23 to 3.44) with possible risk values (lower than 1.8) increasing the load, and also an important oscillation in surge margin (possible risks in other transient phases). So, even if the coupling of PI controllers with a feed-forward approach can produce interesting results, the correct behaviour of the plant (preventing risks) is obtained when a smoothing device is connected on the electrical side (a battery or connection to an external grid), as shown in Fig.1.

4.2. Load Step Increase

A second transient response tested with this new control system is a load step increase. To carry out a comparison with the previous control approach proposed in [33], a 5% step increase was considered starting from about 256.3 kW hybrid system load (90% of design value). At time 0, the electrical demand was increased with a step to about 270.6 kW (95% of design value) and the simulation was completed when system reached a new steady-state condition. As shown in [33], feedback-based controlling approaches cannot prevent temperature increase peaks because the rotational speed set-point increase is obtained with a measured temperature (in [33] anodic recirculation temperature was used) higher than the set-point. In case this variation is significant (in Fig.13 the PI approach shows a 13.6 K increase), the stack can be damaged (if maximum temperature constraints is exceeded) also at low thermal gradients conditions. On the other hand, a feed-forward approach can produce the necessary coupling between fuel cell load and machine rotational speed especially if a battery is used to smooth effects related to load changes. For these reasons, Fig.13 shows that this new control system can maintain constant SOFC average temperature (Fig.13) also during load step increases avoiding risks due to temperature peaks and stress related to high thermal gradient (always lower than 0.1 K/min with the FF control approach). While results reported in [33] showed a temperature increase which forces to operate the cell with a significant temperature safe margin (from the maximum), Fig.13 shows an almost constant trend obtained with the new approach. Moreover, all the critical parameters were maintained by the control system inside safe ranges. In details, STCR minimum value is 2.08 with a significant margin from 1.8 [60], anode-cathode differential pressure has a -8.4 mbar peak, TIT shows a peak at 1092 K maintaining a significant margin from the mGT maximum sustainable value, surge margin decreases with a minimum value of 1.107 that is higher than the design one.

4.3. Ramps for Load and Ambient Conditions

In this final calculation the control system was tested with ramps for ambient conditions (temperature, pressure and humidity) and electrical load considering one hour and a half (5400 seconds). In details, conditions typical of morning operations were reproduced (one new value at the end of every 900 s periods connected with a linear trend): significant temperature and load demand increase (see Fig.14). The other properties (pressure and relative humidity) were managed simulating a good weather morning (Fig.14).

The power values obtained with the model (Fig.15) focus the attention on battery performance, necessary to have this smooth behaviour. During this load increase ramp battery is discharged to satisfy load demand with peaks (up to 14.7 kW). Other results show that this new control system is able to manage the plant avoiding stress and risk conditions. For instance, Fig.16 shows that fuel cell average temperature is maintained almost constant (±1.3 K maximum variation) with a rotational speed increase (from 58234 rpm to 64961 rpm) avoiding high thermal gradients (maximum values less than 0.3 K/min). The other critical properties were maintained inside safe range conditions. For instance, Fig.17 shows that STCR is always higher than 2.6 (significant safe margin from 1.8 [60]) and maximum anode-cathode differential pressure is lower than 10 mbar (considering its absolute value). Moreover, also the other properties, not reported here for sake of brevity, were well controlled inside safe conditions. For instance, TIT maximum peak is about 1100 K (significant safety margin from its maximum value) and Kp is always higher than 1.1 (1.13 minimum value during the test).

5. Conclusions

This work is related to the development and testing of a new advanced control system for hybrid plants with pressurized SOFCs. Even if the calculations are presented considering a stand-alone application, the same approach can be used for grid connected systems where the battery operations are substituted by the electrical grid. The control logic is based on the coupling of PI controllers with feed-forward approaches necessary to avoid significant temperature variation in the cell (responsible of thermal stress problems) and to reduce the peak values of cathode/anode pressure difference and STCR. So, this work is able to demonstrate improved controlling performance for SOFC hybrid systems, in comparison with previous works [29,32,33,41]. In details, the same component models of [33] were used to compare the good performance obtained with this new controller with the results obtained with the old one shown in [33]. The main conclusions and results presented in this paper are:

- This new control strategy is able to improve SOFC temperature management because it is able to maintain almost constant this property, avoiding significant thermal gradients (maximum values lower than 0.2 K/min for a 10% load step decrease).
- The results obtained with the model show that anode-cathode differential pressure can be maintained at sustainable values during transient operations too (maximum values lower than 10 mbar for a 10% load step decrease).
- This new control system can keep all the critical properties inside safe conditions. STCR, turbine TIT and Kp are always calculated with a significant safety margin from critical values. For instance, STCR minimum value is 2.18 in the 10% load step decrease, while its limit value is usually 1.8 [60].
- The tests carried out considering ramp variations in load and ambient conditions proved that typical plant operations can be tolerated by this new advanced control system with good performance (ramp test main results: thermal gradient in the cell lower than 0.3 K/min, anode-cathode differential pressure lower than 10 mbar, STCR minimum value higher than 2.05).

Additional activities are being developed at TPG on hybrid system controllers. More specifically, an emulator plant [61] is being operated to test control approaches in hardware-in-the-loop configuration, considering not only traditional approaches, but also innovative ones (e.g. model predictive control logics [62], which is considered promising in co-generative plants [63]).

Acknowledgements

The author would like to thank Prof. Aristide F. Massardo, TPG Coordinator, for his essential scientific support and Prof. Alberto Traverso, the main developer of TRANSEO tool.

Nomenclature

Acronyms	
AC	Ambient Conditions
DOE	Department Of Energy
DS	DeSulfurizer
FC	Fuel Cell
FF	Feed-Forward
HS	Hybrid System
mGT	micro Gas Turbine
NETL	National Energy Technology Laboratory
PI	Proportional-Integral controller
REC	RECuperator
SOFC	Solid Oxide Fuel Cell
TPG	Thermochemical Power Group
Variables	
Coeff	power sharing-out coefficient [-]
diff_p	anode-cathode differential pressure [Pa]
eff	plant net efficiency [-]
FO	valve Fractional Opening [-]
LHV	Low Heating Value [J/kg]
Kp	surge margin [-]
K_p	proportional coefficient for a PI controller [-]
i	electrical current density [A/m^2]
m	mass flow rate [kg/s]
n	molar flow rate [mol/s]
N	rotational speed [rpm]
p	pressure [Pa]
P	power [W]
RH	Relative Humidity [%]
STCR	Steam-To-Carbon Ratio [-]
T	temperature [K]
Ta	ambient temperature [K]
TIT	Turbine Inlet Temperature [K]
U_f	fuel utilization factor [-]
XMA	mass fraction [-]
Greek symbols	
β	compression ratio
τ_I	integral coefficient for a PI controller [-]
Subscripts	
ar	anodic recirculation
aux	auxiliaries

cath	cathodic
dp	design point
f	fuel
FC	Fuel Cell
in	inlet
mGT	micro Gas Turbine
out	outlet
s.l.	surge line

References

[1] Yan J., Chou S.K., Desideri U., Xia X., Innovative and sustainable solutions of clean energy technologies and policies (Part I). Applied Energy 130 (2014) 447-449.

[2] Komatsu Y., Brus G., Kimijima S., Szmyd J.S, The effect of overpotentials on the transient response of the 300W SOFC cell stack voltage. Applied Energy 115 (2014) 352-359.

[3] Ferrari M.L., Traverso A., Pascenti M., Massardo A.F, Plant Management Tools Tested With a Small-Scale Distributed Generation Laboratory. Energy Conversion and Management, 78 (2014) 105–113.

[4] Iora P., Silva P., Innovative combined heat and power system based on a double shaft intercooled externally fired gas cycle, Applied Energy 105 (2013) 108-115.

[5] Yan J., Chou S.K., Desideri U., Tu S.T., Jin H.G., Research, development and innovations for sustainable future energy systems. Applied Energy 112 (2013) 393-394.

[6] Rivarolo M., Bellotti D., Mendieta A., Massardo A.F., Hydro-methane and methanol combined production from hydroelectricity and biomass: Thermo-economic analysis in Paraguay. Energy Conversion and Management 79 (2014) 74-84.

[7] Leung D.Y.C., Yang H., Yan J., Novel studies on hydrogen, fuel cell and battery energy systems. International Journal of Energy Research 35 (2011) 1.

[8] Ferrari M.L., Pascenti M., Traverso A.N., Massardo A.F., Hybrid System Test Rig: Chemical Composition Emulation With Steam Injection. Applied Energy Vol. 97 (2012) 809–815.

[9] Lee K.H., Woo H.T., Lee S.M., Lee Y.D., Kang S.G., Ahn K.Y., Yu S.S., A Case study of different configurations for the performance analysis of solid oxide fuel cells with external reformers, Transactions of the Korean Society of Mechanical Engineers 36 (2012) 343–350.

[10] Duan L., Huang K., Zhang X.,Yang Y., Comparison study on different SOFC hybrid systems with zero-CO_2 emission. Energy 58 (2013) 66-77.

[11] Wongchanapai S., Iwai H., Saito M., Yoshida H., Performance evaluation of a direct-biogas solid oxide fuel cell-micro gas turbine (SOFC-MGT) hybrid combined heat and power (CHP) system. Journal of Power Sources 223 (2013) 9–17.

[12] Nishino T., Szmyd J.S., Numerical analysis of a cell-based indirect internal reforming tubular SOFC operating with biogas. Journal of Fuel Cell Science and Technology 7 (2010) 051004_1-8.

[13] Liso V., Olesen A.C., Nielsen, M.P., Kær, S.K., Performance comparison between partial oxidation and methane steam reforming processes for solid oxide fuel cell (SOFC) micro combined heat and power (CHP) system. Energy, 36 (2011) 4216-4226.

[14] Calì M., Santarelli M.G.L., Leone P., Design of experiments for fitting regression models on the tubular SOFC CHP 100 kW_e: Screening test, response surface analysis and optimization. International Journal of Hydrogen Energy 32 (2007) 343-358.

[15] Milewski J., Miller A., Sałaciński J., Off-design analysis of SOFC hybrid system. International Journal of Hydrogen Energy 32 (2007) 687-698.

[16] Bergaentzlé C., Clastres C., Khalfallah H., Demand-side management and European environmental and energy goals: An optimal complementary approach. Energy Policy, 67 (2014) 858-869.

[17] Miller A., Milewski J., Salacinski J., Off-design Operation of Fuel Cell – Gas Turbine Hybrid System. Seventh European Conference on Turbomachinery – Fluid Dynamics and Thermodynamics (2010) 699-715.

[18] Nanaeda K., Mueller F., Brouwer J., Samuelsen S., Dynamic modeling and evaluation of solid oxide fuel cell – combined heat and power system operating strategies. Journal of Power Sources 195 (2010) 3176–85.

[19] Ghigliazza F, Traverso A, Massardo AF, Wingate J, Ferrari ML. Generic Real-Time Modeling of Solid Oxide Fuel Cell Hybrid Systems. Journal of Fuel Cell Science and Technology 6 (2009) 021312_1-7.

[20] Pezzini P, Tucker D, Traverso A. Avoiding compressor surge during emergency shutdown hybrid turbine systems. Journal of Engineering for Gas Turbines and Power 2013;135(10): 102602_1-10.

[21] Hohloch M, Widenhorn A, Lebküchner D, Panne T, Aigner M. Micro gas turbine test rig for hybrid power plant application. ASME Paper GT2008-50443; 2008.

[22] Veyo S., Shockling L.A., Dederer J.T., Gillett J.E., Lundberg W.L., Tubular Solid Oxide Fuel Cell/Gas Turbine Hybrid Cycle Power Systems: Status. Journal of Engineering for Gas Turbines and Power 124 (2002) 845-849.

[23] Otomo J., Oishi J., Mitsumori T., Iwasaki H., Yamada K., Evaluation of cost reduction potential for 1 kW class SOFC stack production: Implications for SOFC technology scenario. International Journal of Hydrogen Energy 38 (2013) 14337-14347.

[24] Bakalis D.P., Stamatis A.G., Incorporating available micro gas turbines and fuel cell: Matching considerations and performance evaluation. Applied Energy, 103 (2013) 607-617.

[25] Zhao H., Dang Z., Xi G., Investigation of coupling characteristics of SOFC/MG hybrid system. Journal of Engineering Thermophysics, 32 (2011) 1647-1650.

[26] Ferrari M.L., Massardo A.F., Cathode-Anode Interaction in SOFC Hybrid Systems. Applied Energy, 105 (2013) 369–379.

[27] Du L.X., Ma T., Zeng M., Guo Z.X., Wang Q.W., Numerical investigations on the thermohydraulic performance of cross-wavy channels with multi-periodic boundary conditions. Numerical Heat Transfer; Part A: Applications, 65 (2014) 732-749.

[28] Massardo A.F., Bosio B., Assessment of molten carbonate fuel cell models and integration with gas and steam cycles. Journal of Engineering of Gas Turbine and Power, 124 (2000) 103-109.

[29] Magistri L., Traverso A., Massardo A.F., Heat exchangers for fuel cell and hybrid system applications. Journal of Fuel Cells Science and Technology, 3 (2006) 111-118.

[30] Santis-Alvarez A.J., Nabavi M., Hild N., Poulikakos D., Stark W.J. A fast hybrid start-up process for thermally self-sustained catalytic n-butane reforming in micro-SOFC power plants. Energy and Environmental Science, 4 (2011) 3041-3050.

[31] McLarty D., Brouwer J., Samuelsen S., Fuel cell gas turbine hybrid system design part II: Dynamics and control. Journal of Power Sources, 254 (2014) 126–136.

[32] McLarty D., Kuniba Y., Brouwer J., Samuelsen S., Experimental and theoretical evidence for control requirements in solid oxide fuel cell gas turbine hybrid systems. Journal of Power Sources 209 (2012) 195-203.

[33] Ferrari ML. Solid Oxide Fuel Cell Hybrid System: Control Strategy for Stand-Alone Configurations. Journal of Power Sources 196 (2011) 2682-2690.

[34] Hawkes A.D., Aguiar P., Croxford B., Leach M.A., Adjiman C.S., Brandon N.P., Solid oxide fuel cell micro combined heat and power system operating strategy: Options for provision of residential space and water heating. Journal of Power Sources, 164 (2007) 260–271.

[35] Henke M., Willich C., Westner C., Leucht F., Kallo J., Bessler W.G., Friedrich K.A. A validated multi-scale model of a SOFC stack at elevated pressure. Fuel Cells 13 (2013) 773-780.

[36] Stiller C., Thoruda B., Bolland O., Kandepu R, Lars Imsland L., Control strategy for a solid oxide fuel cell and gas turbine hybrid system. Journal of Power Sources, 158 (2006) 303–315.

[37] Jia Z., Sun J., Oh S.-R., Dobbs H., King J., Control of the dual mode operation of generator/motor in SOFC/GT-based APU for extended dynamic capabilities, Journal of Power Sources, 235 (2013) 172-180.

[38] Wua X.-J., Zhub X.-J., Multi-loop control strategy of a solid oxide fuel cell and micro gas turbine hybrid system. Journal of Power Sources, 196 (2011) 8444–8449.

[39] Rao S.M.V., Jagadeesh G., Novel supersonic nozzles for mixing enhancement in supersonic ejectors. Applied Thermal Engineering 71 (2014) 62-71.

[40] M.L. Ferrari, M. Pascenti, L. Magistri, A.F. Massardo, Hybrid System Test Rig: Start-up and Shutdown Physical Emulation, J. Fuel Cell Science and Technology 7 (2010) 021005_1-7.

[41] Barelli L., Bidini G., Ottaviano A., Part load operation of a SOFC/GT hybrid system: Dynamic analysis. Applied Energy 110 (2013) 173–189.

[42] Ferrari M.L., Pascenti M., Massardo A.F., Ejector Model for High Temperature Fuel Cell Hybrid Systems: Experimental Validation at Steady-State and Dynamic Conditions. Journal of Fuel Cell Science and Technology, 5 (2008) 041005_1-7.

[43] Ferrari M.L., Liese E., Tucker D., Lawson L., Traverso A., Massardo A.F., Transient Modeling of the NETL Hybrid Fuel Cell/Gas Turbine Facility and Experimental Validation. Journal of Engineering for Gas Turbines and Power, 129 (2007) 1012-1019.

[44] Ferrari M.L., Traverso A., Magistri L., Massardo A. F., Influence of the Anodic Recirculation Transient Behaviour on the SOFC Hybrid System Performance. Journal of Power Sources, 149 (2005) 22-32.

[45] Traverso A., TRANSEO Code for the Dynamic Simulation of Micro Gas Turbine Cycles. ASME Paper 2005-GT-68101, 2005.

[46] Traverso A., TRANSEO: a New Simulation Tool for Transient Analysis of Innovative Energy Systems, Ph.D. Thesis, TPG-DiMSET, University of Genoa, 2004.

[47] Traverso A., Trasino F., Magistri L., Massardo A.F., Time Characterisation of the Anodic Loop of a Pressurized Solid Oxide Fuel Cell System, J. Engineering for Gas Turbines and Power, 130 (2008) 021702_1-9.

[48] Traverso A., Calzolari F., Massardo A.F., Transient Behavior of and Control System for Micro Gas Turbine Advanced Cycles Based on Microturbine Technology. Journal for Engineering of Gas Turbine and Power 127 (2005) 340-347.

[49] Singhal S.C., Advances in Solid Oxide Fuel Cell Technology. Solid State Jonics, 135 (2000) 305-313.

[50] Magistri L., Bozzo R., Costamagna P., Massardo A.F., Simplfied versus detailed SOFC reactor models and influence on the simulation of the design point performance of hybrid system. ASME Paper 2002 GT-30653.

[51] Magistri L., Trasino F., Costamagna P., Transient Analysis of Solid Oxide Fuel Cell Hybrids Part I: Fuel Cell Models. Journal of Engineering of Gas Turbine and Power, 128 (2006) 288-293.

[52] Zheng H.T., Cai L., Li Y.J., Li Z.M., Computational fluid dynamics simulation of the supersonic steam ejector. Part 1: Comparative study of different equations of state. Proceedings of the Institution of Mechanical Engineers, Part C: Journal of Mechanical Engineering Science, 226 (2012) 709-714.

[53] Zhu Y., Cai W., Li Y., Wen C., Anode gas recirculation behavior of a fuel ejector in hybrid solid oxide fuel cell systems: Performance evaluation in three operational modes. Journal of Power Sources, 185 (2008) 1122-1130.

[54] Brunner D.A., Marcks S., Bajpai M., Prasad A.K., Advani S.G., Design and characterization of an electronically controlled variable flow rate ejector for fuel cell applications. International Journal of Hydrogen Energy, 37 (2012) 4457-4466.

[55] Ferrari M.L., Traverso A., Pascenti M., Massardo A.F., Early Start-up of SOFC Hybrid Systems with Ejector Cathodic Recirculation: Experimental Results and Model Verification. Proceedings of the Institution of Mechanical Engineers, Part A, Journal of Power and Energy, 221 (2007) 627-635.

[56] McLarty D., Brouwer J., Samuelsen S., Fuel cell-gas turbine hybrid system design part I: Steady state performance. Journal of Power Sources, 257 (2014) 412-420.

[57] Jan Zanger J., Widenhorn A., Aigner M., Experimental Investigations of Pressure Losses on the Performance of a Micro Gas Turbine System. Journal of Engineering for Gas Turbines and Power, 133 (2011) 082302_1-9.

[58] Traverso A., Massardo A.F., Scarpellini R., Externally Fired micro-Gas Turbine: Modelling and Experimental Performance. Applied Thermal Engineering, 26 (2006) 1935-1941.

[59] Kurfess T.R., Getting in tune with Ziegler-Nichols. Control Engineering, 54 (2007), 28.

[60] Marsano F., Magistri L., Massardo A.F., Ejector performance influence on a solid oxide fuel cell anodic recirculation system. Journal of Power Sources, 129 (2004) 216-228.

[61] Ferrari M.L., Pascenti M., Magistri L., Massardo A.F., MGT/HTFC Hybrid System Emulator Test Rig: Experimental Investigation on the Anodic Recirculation System. Journal of Fuel Cell Science and Technology, 8 (2011) 021012_1-9.

[62] Larosa L., Traverso A., Ferrari M.L., Zaccaria V., Pressurized SOFC Hybrid Systems: Control System Study and Experimental Verification. Journal of Engineering for Gas Turbines and Power, 137 (2015) 031602_1-8.

[63] Kortela J., Jämsä-Jounela S.-L., Model predictive control utilizing fuel and moisture soft-sensors for the BioPower 5 combined heat and power (CHP) plant. Applied Energy, 131 (2014) 189-200.

Figures and Tables

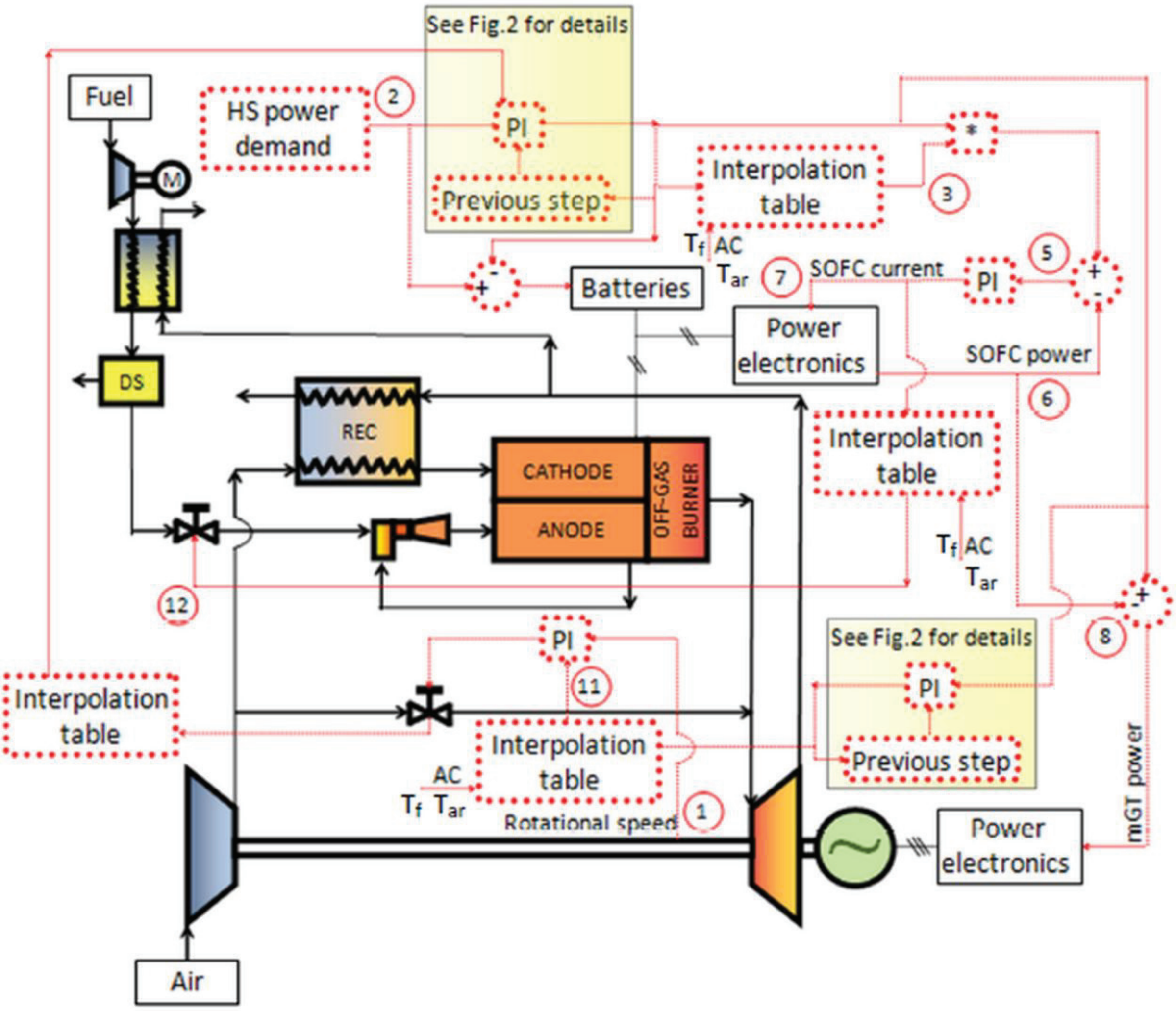

Figure 1. Plant and control system layouts.

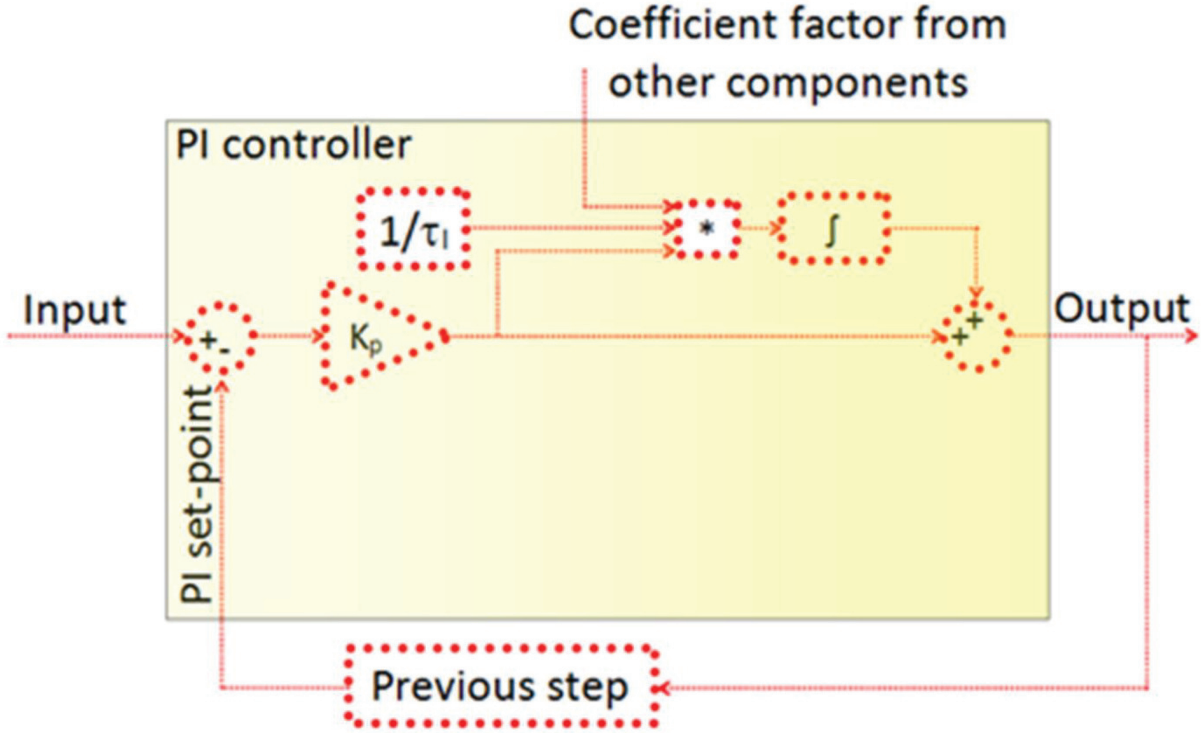

Figure 2. Diagram of PI controller including the previous step block.

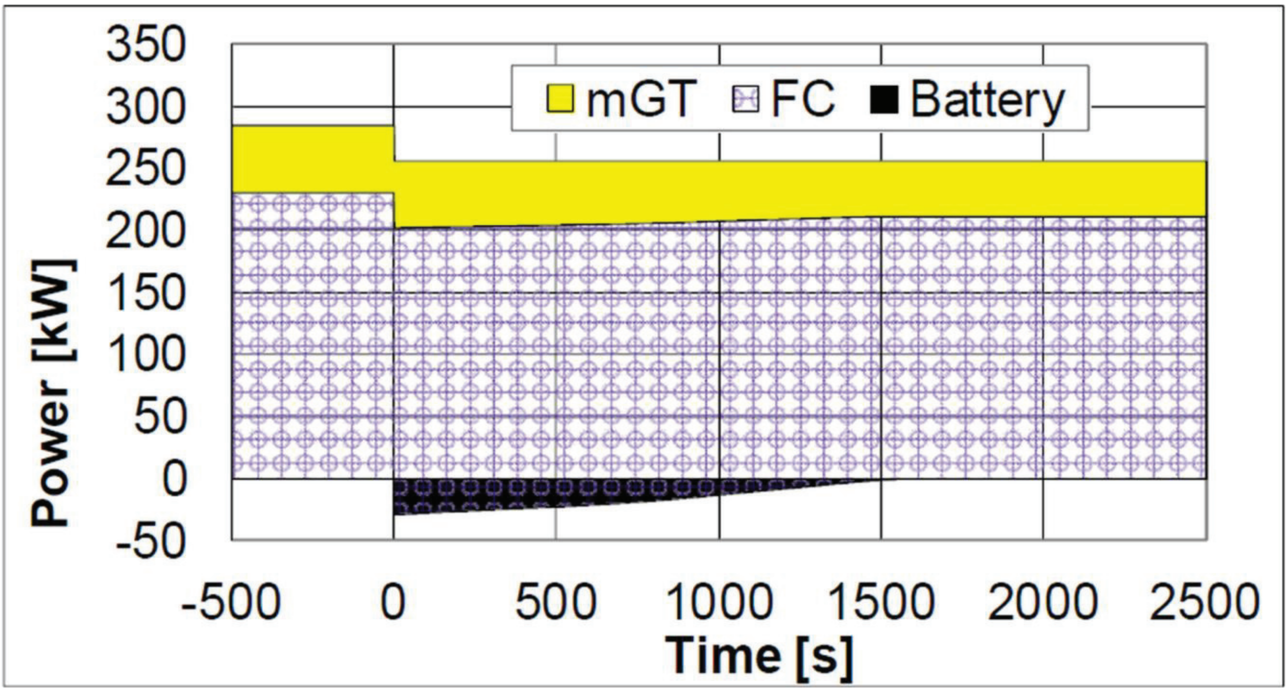

Figure 3. 10% load step decrease: electrical power produced by FC and mGT coupled with battery charging (negative values).

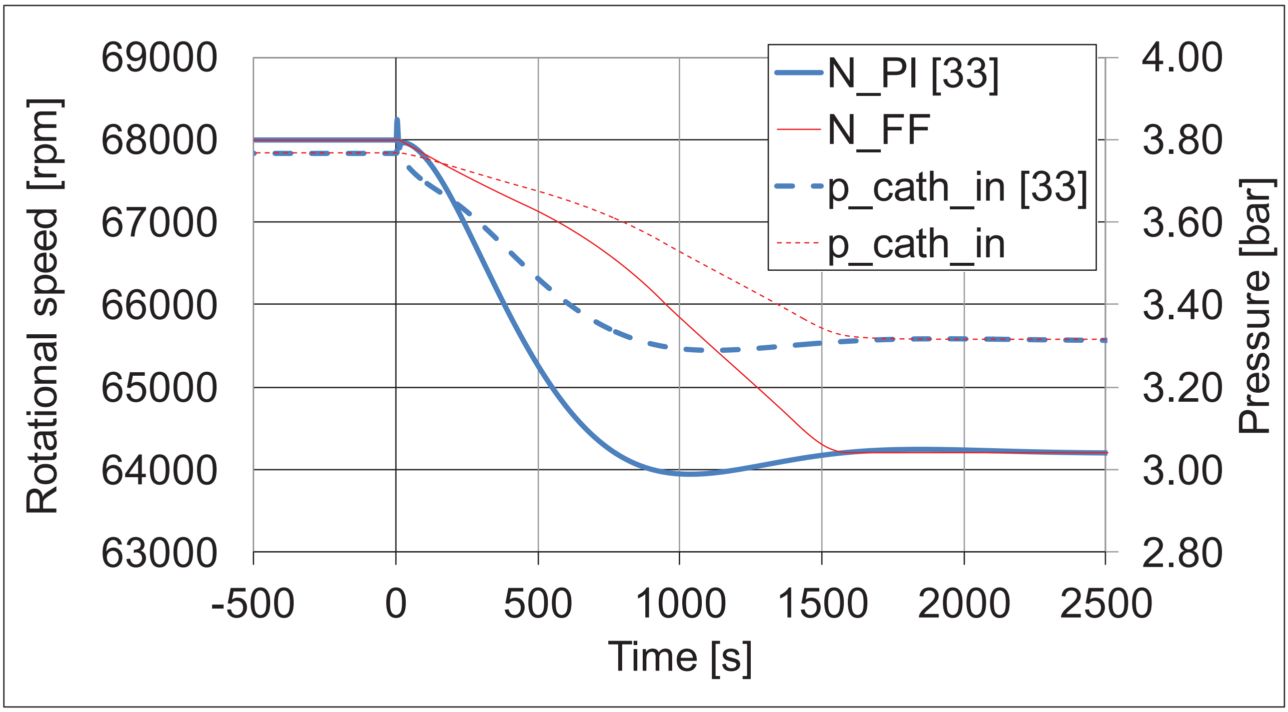

Figure 4. 10% load step decrease: rotational speed and cathode inlet pressure compared to previous results [33].

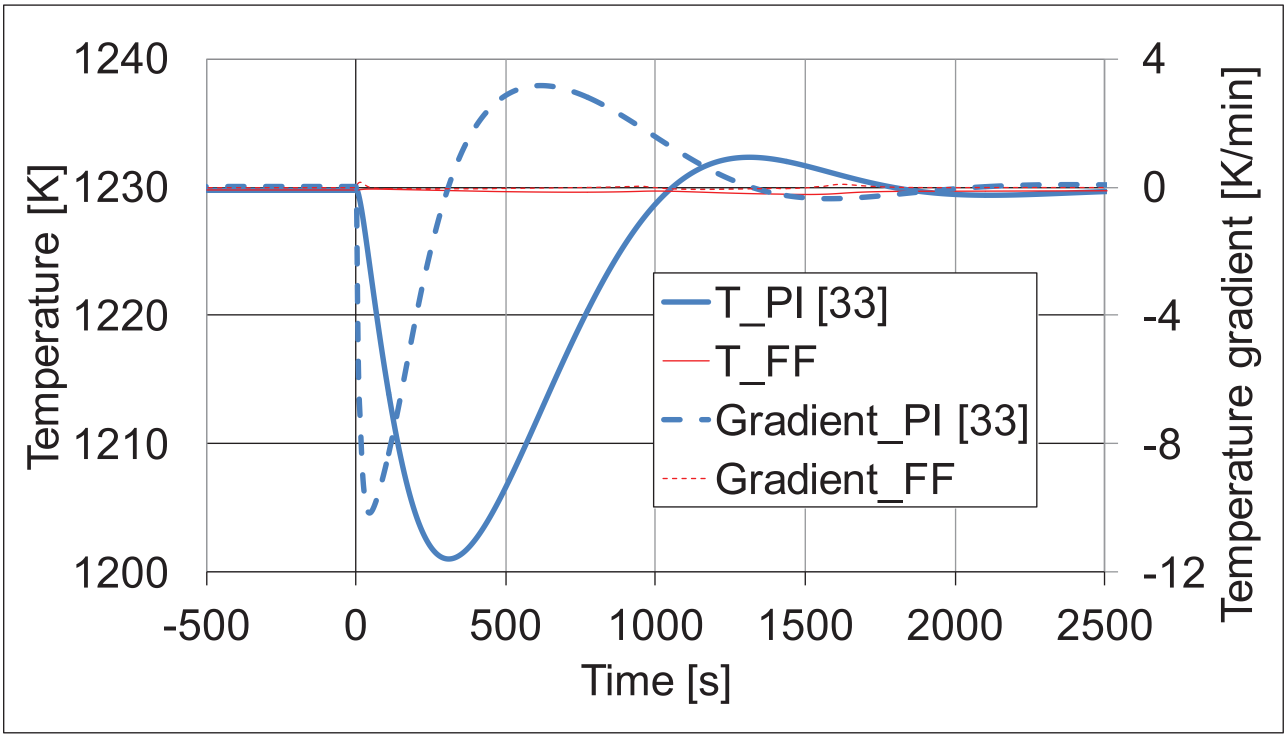

Figure 5. 10% load step decrease: SOFC average temperature, including temperature gradient, compared to previous results [33].

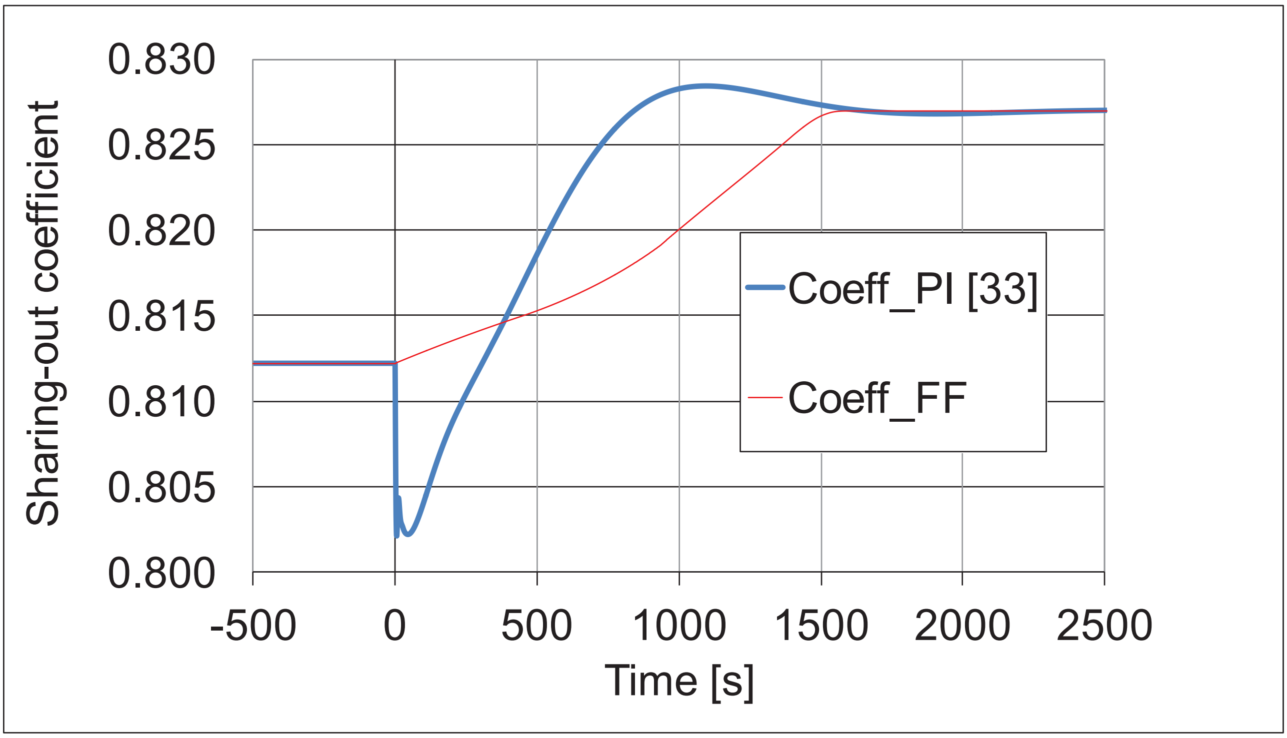

Figure 6. 10% load step decrease: power sharing-out coefficient compared to previous results [33].

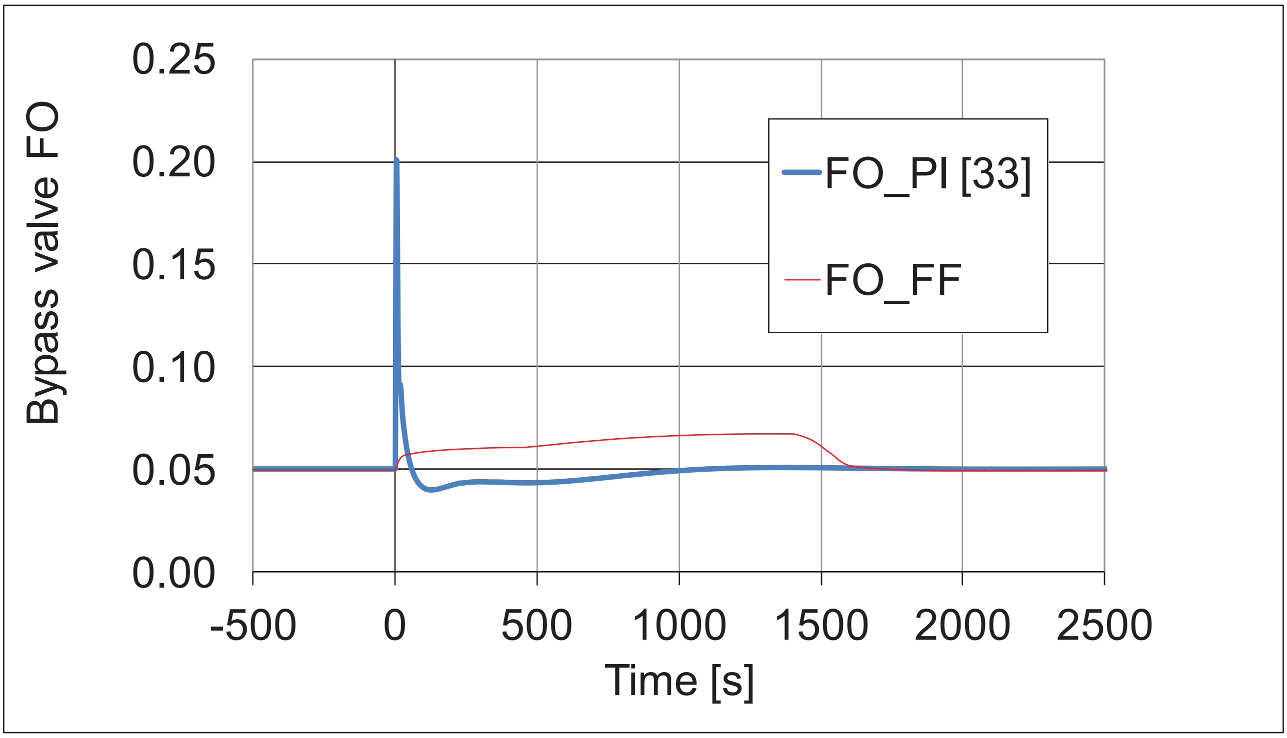

Figure 7. 10% load step decrease: bypass valve FO compared to previous results [33].

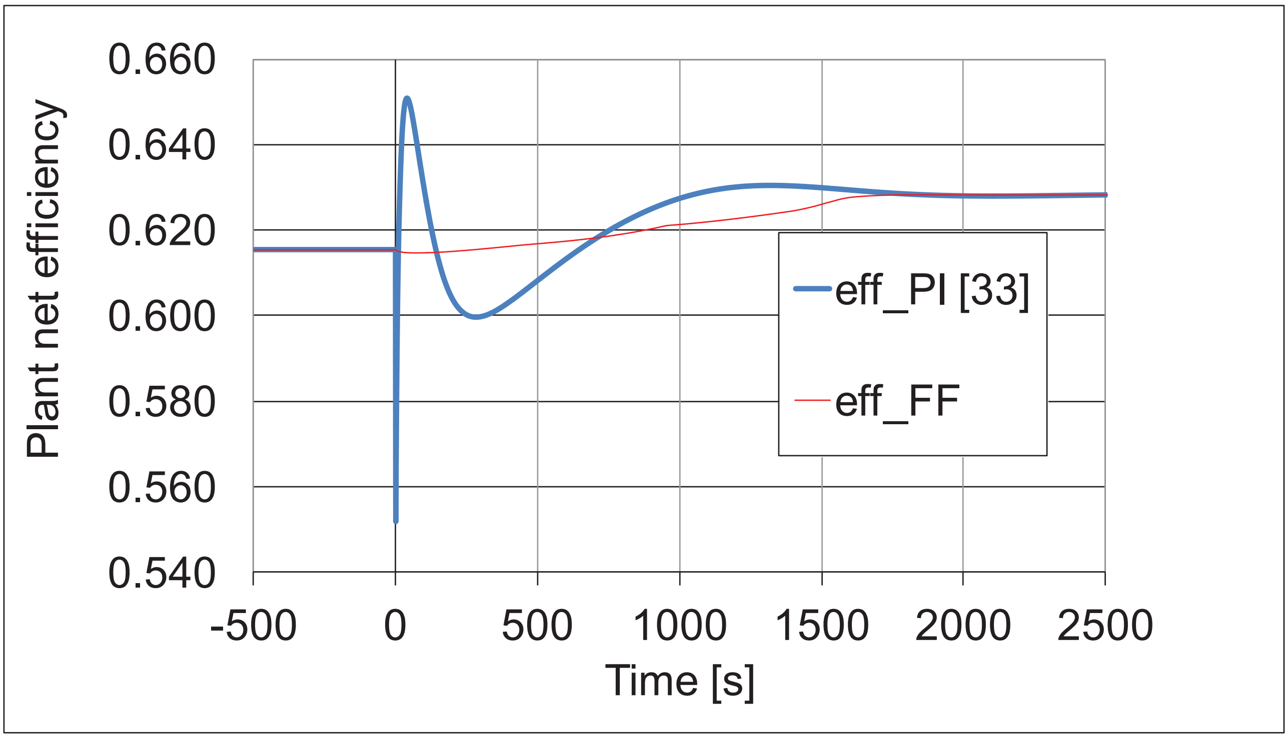

Figure 8. 10% load step decrease: plant net efficiency compared to previous results [33].

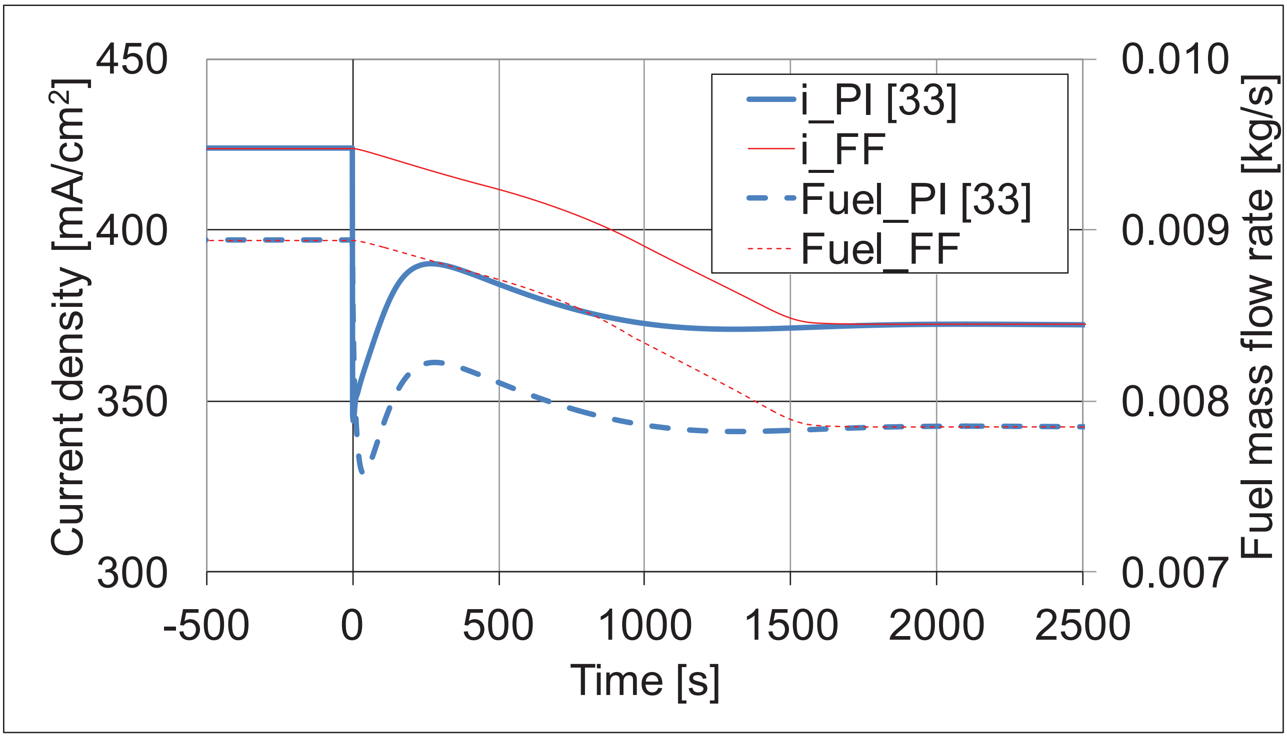

Figure 9. 10% load step decrease: fuel cell current density and fuel mass flow rate in the ejector primary duct compared to previous results [33].

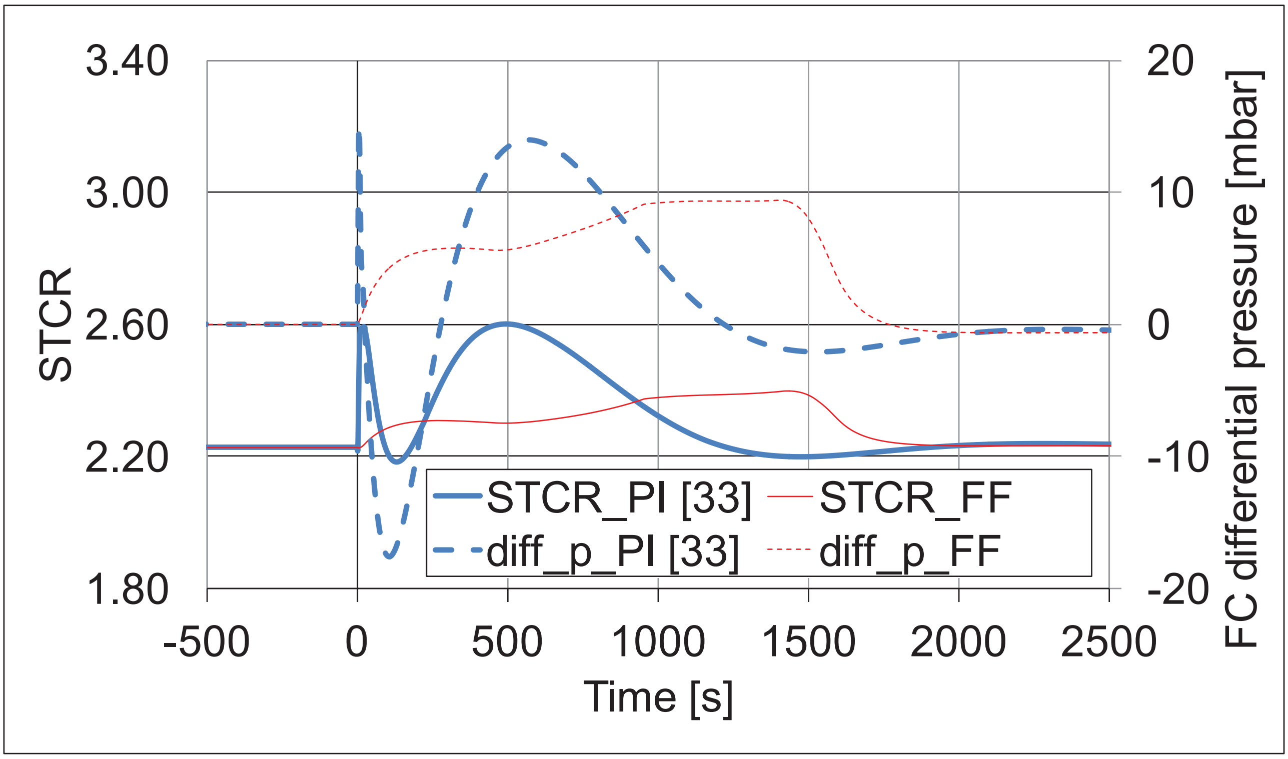

Figure 10. 10% load step decrease: fuel cell STCR and fuel cell differential pressure (between anode and cathode sides) compared to previous results [33].

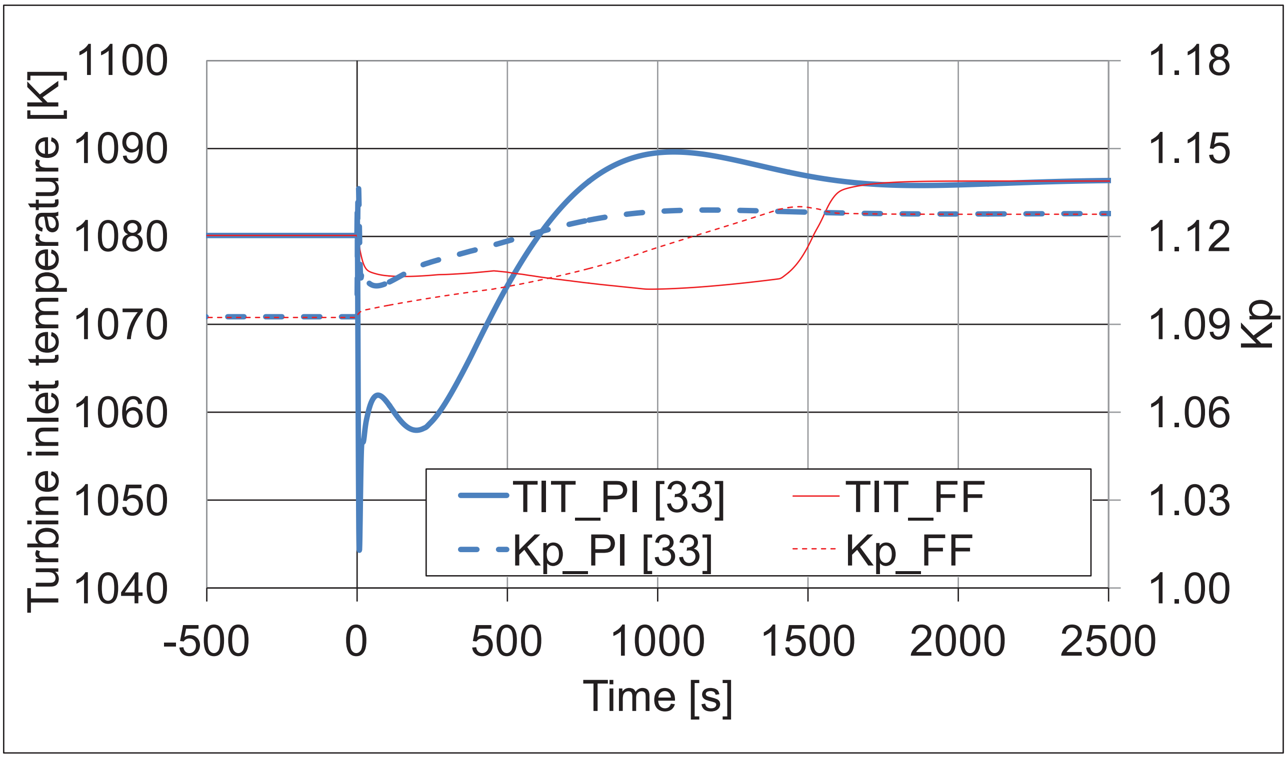

Figure 11. 10% load step decrease: TIT and compressor surge margin (Kp) compared to previous results [33].

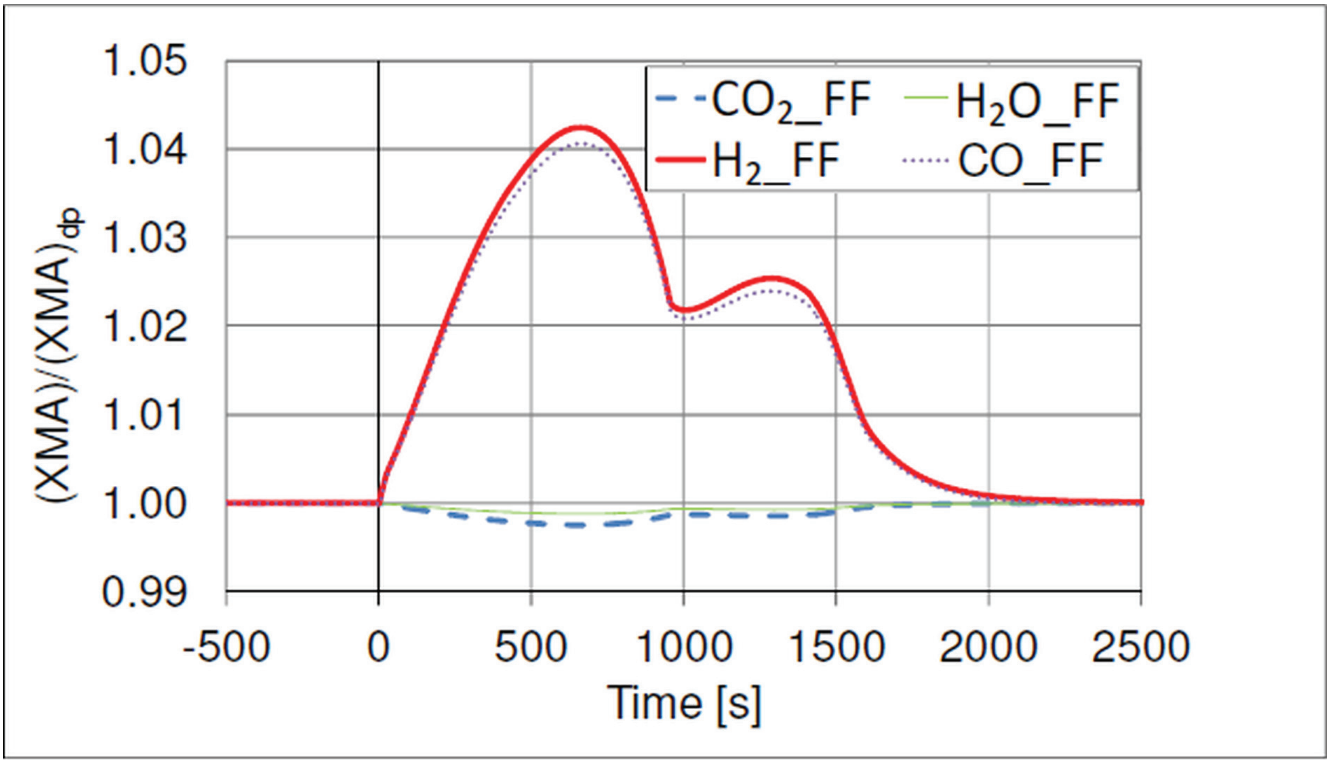

Figure 12. 10% load step decrease: mass fractions of anodic outlet flow (referenced to their design values) for this new control system (FF).

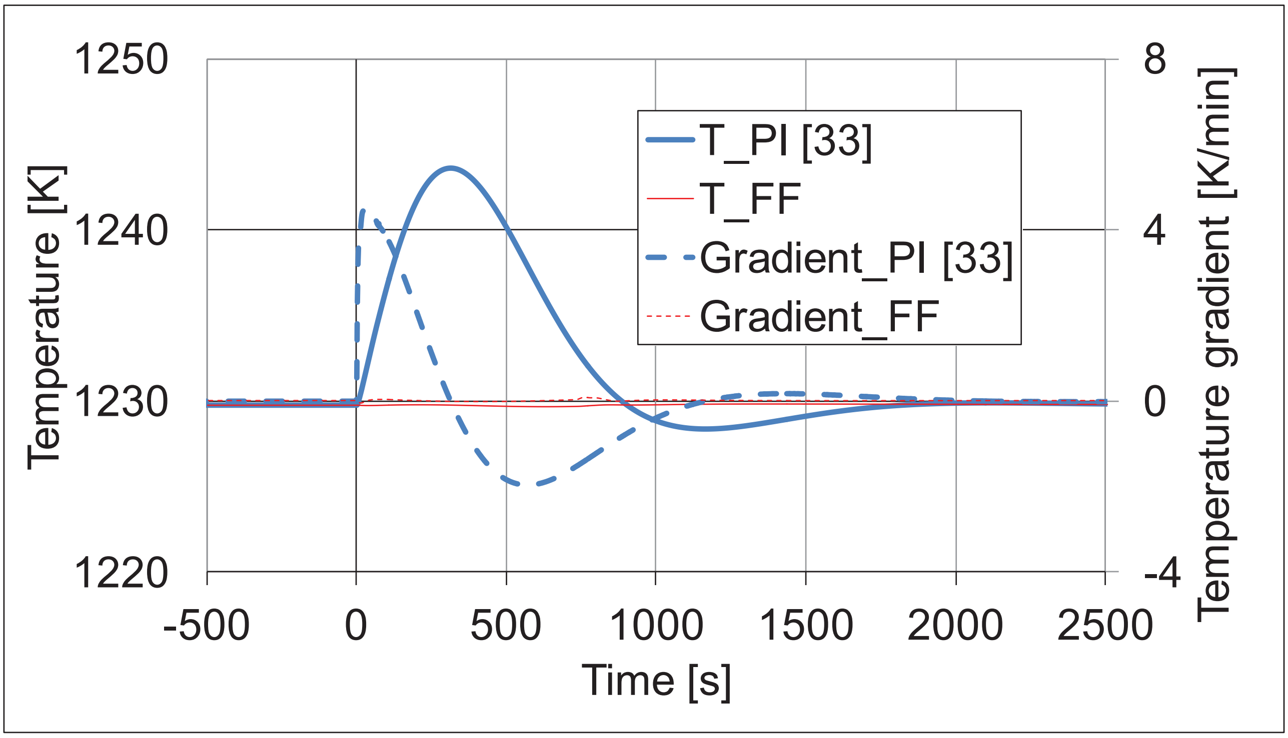

Figure 13. 5% load step increase: SOFC average temperature, including temperature gradient, compared to previous results [33].

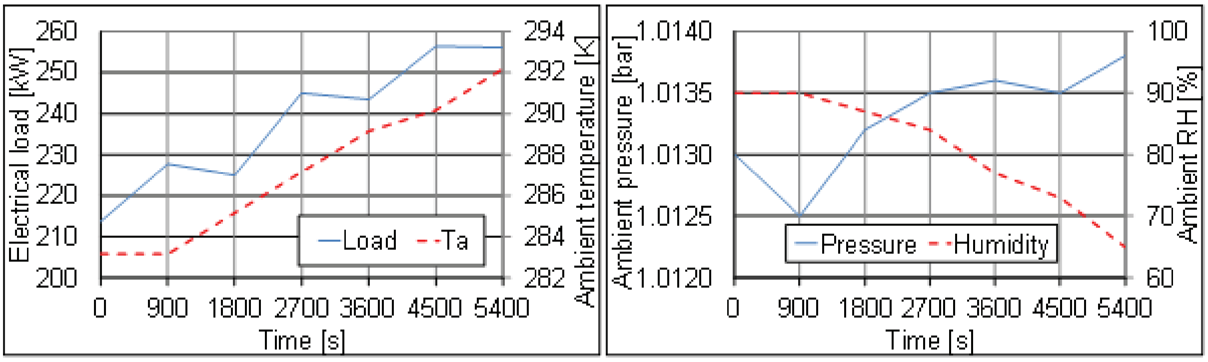

Figure 14. Ramps for load and ambient conditions: input values.

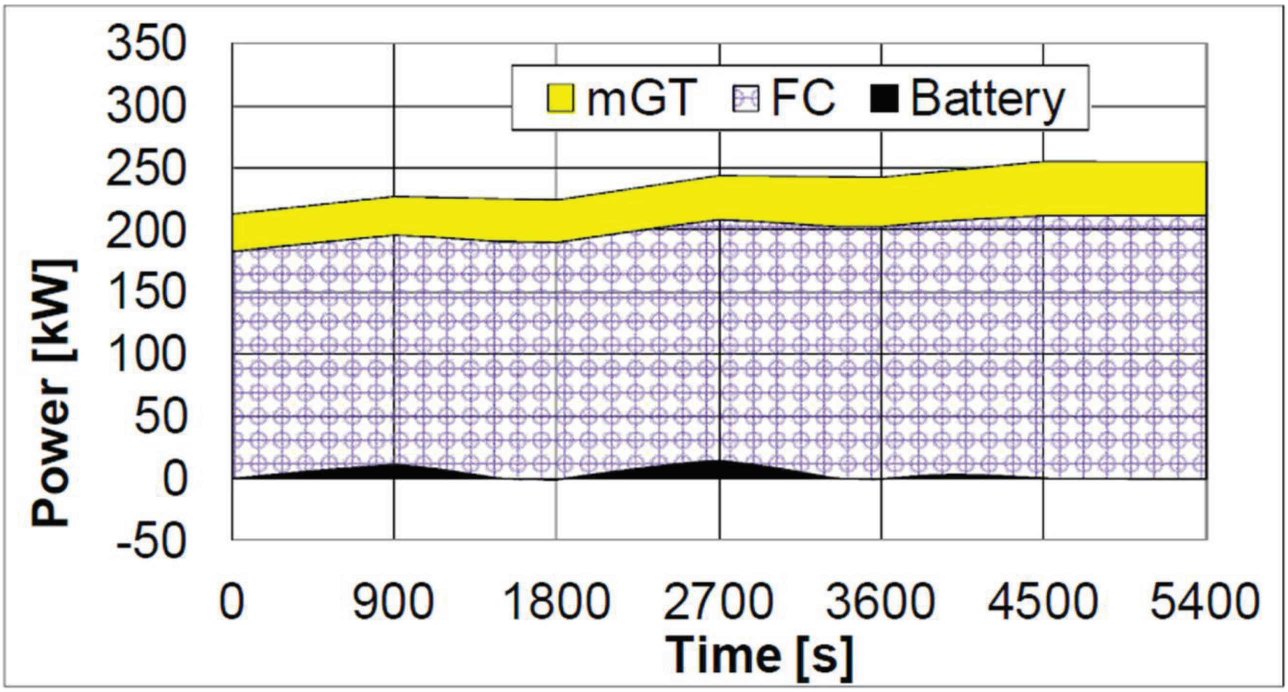

Figure 15. Ramps for load and ambient conditions: electrical power produced by FC and mGT coupled with battery charging (negative values).

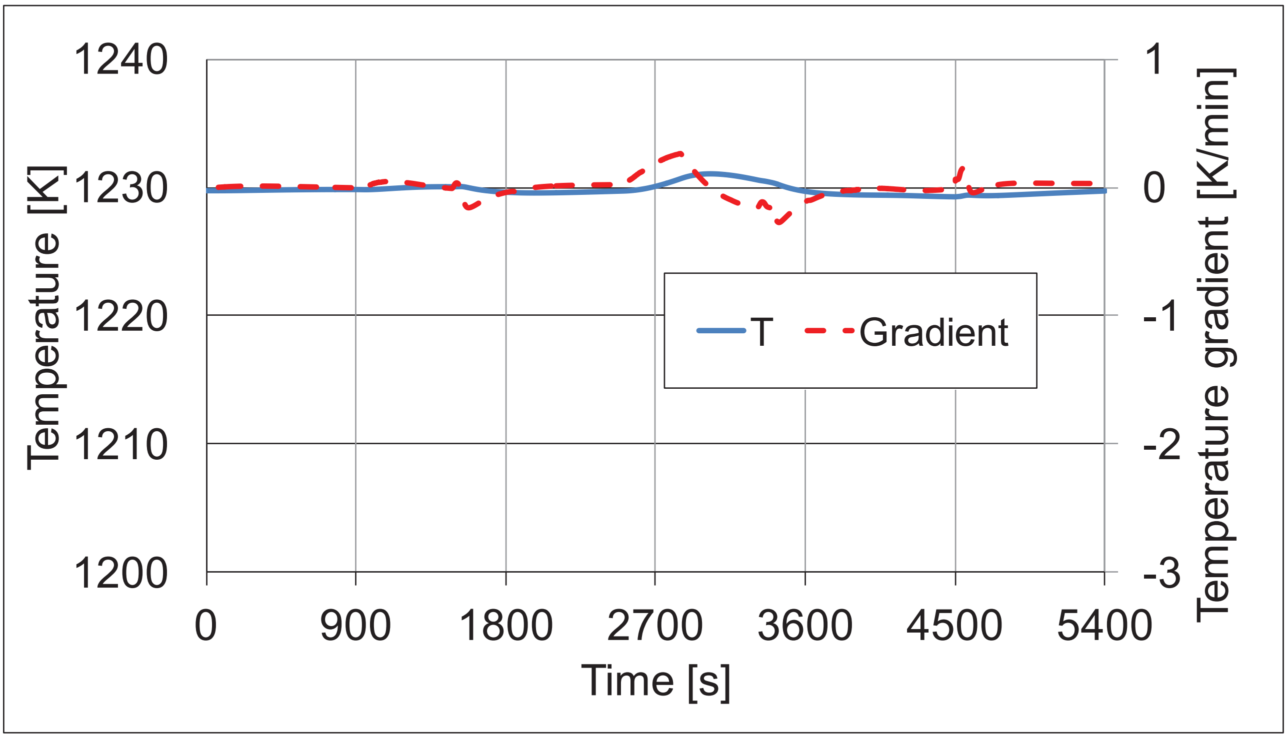

Figure 16. Ramps for load and ambient conditions: SOFC average temperature and the related gradient.

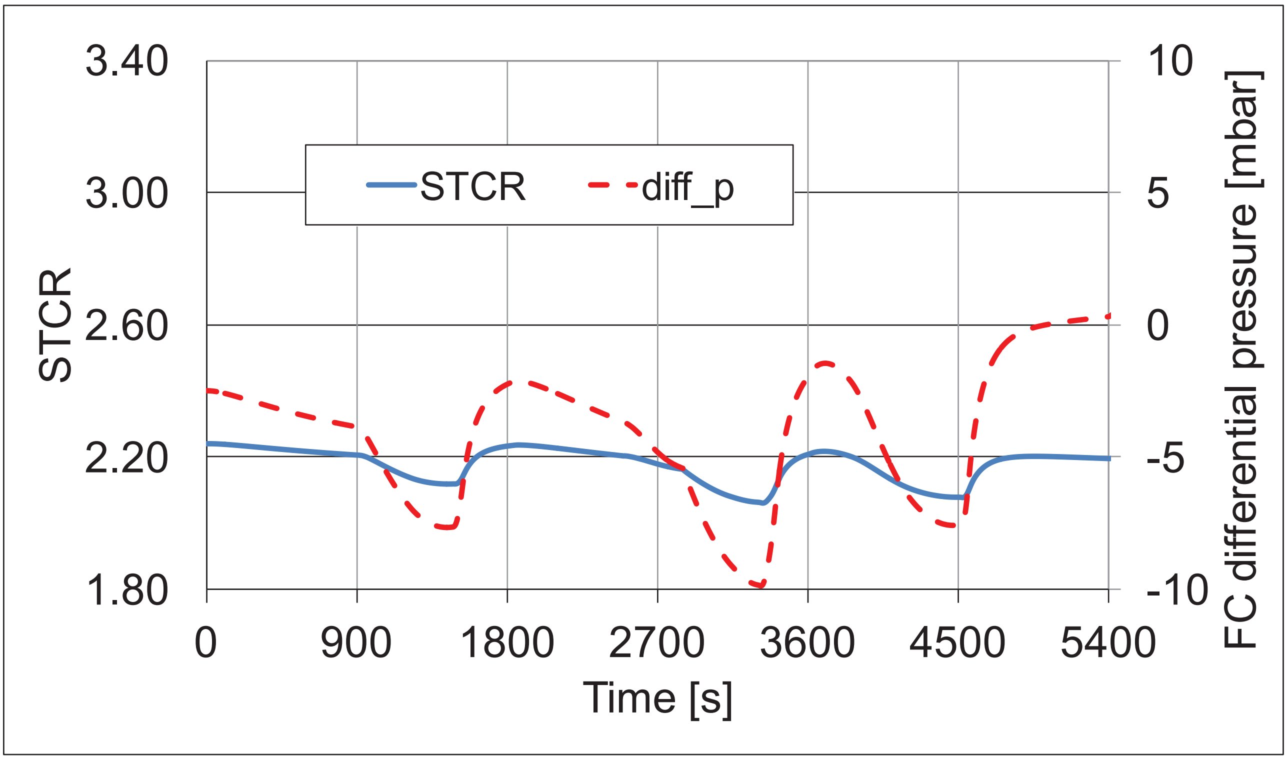

Figure 17. Ramps for load and ambient conditions: fuel cell STCR and fuel cell differential pressure (between anode and cathode sides).